Structural, Electrochemical and Catalytic Elucidation of Cyclooctadiene Ru(II)-Nitrile Complexes of the Type $[RuCl_2(cod)(NCR)_2]$

Frederick P. Malan*[a]

[a] Dr FP Malan
Department of Chemistry
University of Pretoria
Lynnwood road, Hatfield, Pretoria, 0002
E-mail: frikkie.malan@up.ac.za

Supporting information for this article is given via a link at the end of the document.

Abstract The facile synthesis of a range of eleven cyclooctadiene Ru(II) complexes of the type $[RuCl_2(cod)(NCR)_2]$ featuring different nitrile ligands using two synthetic routes is reported. The solid-state characterization (SCXRD) of twelve complexes is also described. Complex instability in solution led to spontaneous dimerization to yield a dimeric complex. Using these complexes, varied catalytic activity was observed in six different transformation reactions, of which the transfer hydrogenation of ketones was the highest (yields of 99% after 30 minutes, TOF = 156 h^{-1}). The electrochemical (CV), DFT, and catalytic properties of the complexes evaluated showed that while the majority of the characteristics of the complexes are comparable, three complexes stood out with the lowest catalytic activity (16% and lower), the highest (most positive) formal redox potentials for Ru^{II}/Ru^{III} ($E^{0'}$ of up to +1.4 V), as well as exhibiting some of the smallest energy gaps (as small as 1.21 eV) in the series.

Introduction

Transition metal complexes featuring functionalized nitrile ligands remain an important class of compounds that are studied in light of the associated catalytic properties imparted in the complexes due to the resultant change in the electrophilicity or nucleophilicity of the ligand upon coordination.[1, 2] This is in part due to their moderate σ-donating and weak π-accepting properties, as well as them belonging to the important dissociable solvent ligand class, which allow for rapid ligand substitution to afford new coordination and organometallic compounds.[1-3] Complexes featuring organonitriles may also serve as models for systems capable of small molecule activation including nitrogen fixation, due to the RCN group being isoelectronic with molecular nitrogen, carbon monoxide, isocyanides and alkynyls.[1, 4] The chemical versatility that the transformation of the nitrile ligand offers is often only accessible when coordinated to metal ions in nucleophilic and electrophilic forms of activation.[5] Examples illustrating the functional use of nitrile ligands with ruthenium as metal are relatively scarce, with the formation of metallacycles *via* the nucleophilic reduction of nitriles being the most interesting.[5(a)] Hiraki *et al.*[6] demonstrated how the hydrido Ru(II) complex $[RuHCl(CO)(PPh_3)_3]$ couples two molecules of aromatic nitriles to form the ruthenacycles $[RuCl(CO)(PPh_3)_2(HNC(Ar)NC(Ar)O)]$ in the presence of water. López *et al.*[7] reported the intramolecular coupling of pyrazole derivatives and coordinated nitrile ligands in the ruthenium hydride and alkenyl complexes of $[RuX(CO)(NCR)_2(PPh_3)_2]^+$ (X = H, CH=CHR'; R' = Me, Bn) to form the corresponding ruthenacyles. Kollipara *et al.*[8] and Jones *et al.*[9] similarly reported on the coupling of pyrazole derivatives with acetonitrile in the presence of the $[(\eta^6\text{-arene})RuCl_2]_2$ dimers (arene = benzene, *p*-cymene) to yield the corresponding ruthenacycles of the type $[(\eta^6\text{-arene})Ru\{NH=CMe(R_2pz)\}(R_2Hpz)]^{2+}$. Very little work on the utilization of ruthenium(II) nitrile complexes featuring supporting diene ligands other than their use as synthetic precursors have been reported. This work therefore aims to gain more insight into the structural and electrochemical aspects of cyclooctadiene (cod) Ru(II) complexes featuring a range of organonitrile ligands, as well as look at their catalytic utility in six different catalytic transformation reactions.

Results and Discussion

Synthesis of the Ru(II) nitrile complexes

In this work it was found that two synthetic routes were feasible to arrive at the Ru(II) nitrile complexes under investigation (Figure 1). In route A the direct and neat reaction of the polymeric Ru(II) precursor with a nitrile (reagent and solvent) at 80 °C for six hours resulted in the formation of complexes **1**-**11** in moderate yields (42-59%), after filtration and work-up.

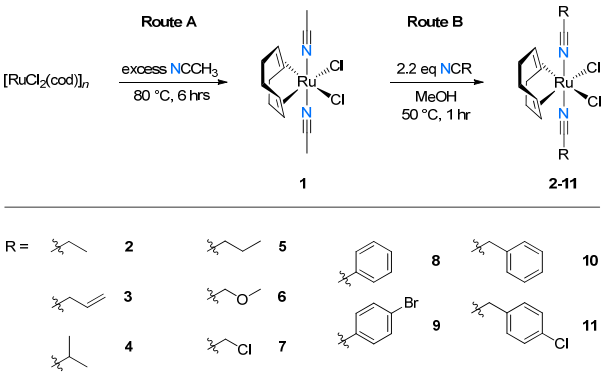

Figure 1. Synthesis of Ru(II) nitrile complexes **1**-**11**.

The nitrile ligands employed were selected based on their steric and electronic properties exhibited, in order to probe the resulting effect on the electrochemical and catalytic activity (*vide infra*) of

the corresponding ruthenium complexes. In contrast, route B allows for the reaction of freshly synthesized **1** with 2.2 equivalents of a nitrile ligand in methanol at 50°C for one hour. After reaction workup, concentration and cooling of the resulting solution, the resulting complexes were obtained in high yields (83-96%). The nitrile complexes **1**-**11** were isolated as pale yellow to orange microcrystalline solids that were found to be bench stable for several months and soluble in most common organic solvents. The NMR spectra of complexes **1**-**11** in general exhibit similar features: (i) the cyclooctadiene ligand in these complexes is symmetrically coordinated to give rise to two sets of aliphatic signals in their ^{1}H NMR spectra between δ_H 1.85-2.14 and 2.22-2.56 ppm. The effect of the nitrile ligands is more visible with the diene signals appearing in general between δ_H 4.17-4.46 ppm. The most upfield signal (δ_H 4.17 ppm) corresponds to the more electron-donating isopropyl substituent, whereas the most downfield signal corresponds to the more electron-withdrawing 4'-Br-phenyl substituent; (ii) The ^{13}C NMR spectra exhibit signals for the aliphatic and diene carbon signals in the ranges δ_C 29.2-31.0 and 89.7-91.1 ppm, respectively. A slight effect of the substituent on the nitrile carbon signal was observed in the corresponding ^{13}C signals, as it appeared in the narrow range of δ_C 126.5-132.6 ppm, although no direct relationship between the type of substituent and ^{13}C signal could be established.

As part of the process of NMR data collection and crystal growth, it was noticed that the stability of the complexes in solution was also limited. In general, solutions of the complexes in $(CH_3)_2CO$, CH_2Cl_2, $CHCl_3$, and Et_2OAc react in a dimerization reaction over the course of several hours to form the corresponding dimeric products [{Ru(cod)(NCR)}(μ_2-Cl)$_3${RuCl(cod)}] (Figure 2). As reported previously by Pérez-Torrente *et al.*[3], this spontaneous dimerization reaction shows first-order kinetic behaviour, where complexes featuring bulky nitrile ligands (e.g. NCPh, complex **8** in this study) dimerize ~10 times slower than corresponding complexes with smaller nitrile ligands (e.g. NCMe, complex **1** in this study). It is also important to note that this reaction is reversible, and in the presence of an excess of nitrile ligands the trichloro-bridge is cleaved to form the corresponding [$RuCl_2$(cod)$(NCR)_2$] complexes.[3]

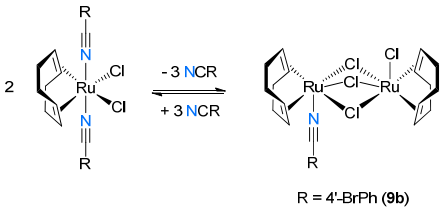

Figure 2. Dimerization reaction of bis-nitrile complexes.

As an example, an EtOAc solution containing complex 9 facilitated a slow dimerization reaction over a period of three days to form crystals of the dimeric complex **9b** in low yield (8%). This complex exhibited stability against light and air in the solid state, and less so against moisture over the course of a few weeks (presumably since aqua ligands may cleave the halogen bridges to form mononuclear by-products). Complex **9b** exhibited lowered solubility in most common organic solvents, however soluble enough for NMR and MS analyses. The ^{1}H NMR spectrum of **9b** was comparable to that of **9**, with aliphatic signals appearing between δ_H 2.06-2.11 and 2.50-2.57 ppm. The unsaturated diene signal appeared as a broad singlet at δ_H 4.42 ppm.

X-ray crystallography

Single crystals of complexes **1**-**11** suitable for diffraction were all obtained from saturated solutions of either di- or trichloromethane, or methanol. The molecular structures of **1**-**9** are shown in Figure 3, along with a summary of key crystallographic parameters (including selected bond distances and angles) in Tables S1-S5 (ESI). An interesting variation on the space groups in which the complexes crystallized in is seen where complexes **1**-**3**, **6**, **7** and **11** all crystallized in the monoclinic $P2_1/x$ (x = m, c, n) space groups, whereas complexes **8** and **9** crystallized in the monoclinic $C2/c$, and complexes **4, 5**, and **9b** in the triclinic space group P-1. Complex **10** is the only complex to have crystallized in the orthorhombic *Pbca*. Complexes **1**, **8**, and **9** all crystallized with half a molecule in the asymmetric unit cell, whereas complexes **2**-**4**, and **6** all contained a full molecule, and complexes **5**, **9b**, **10** and **11** each contained two complete molecules in the asymmetric unit cells. All of the complexes **1**-**11** exhibited slightly distorted octahedral geometries, where the cyclooctadiene, two *cis* dichlorido, and two *trans* nitrile ligands make up the coordination sphere. This distortion is evident from the angles N1-Ru1-Cl1 and Cl1-Ru1-Cl2 that varied between 83.77(7)°-86.68(9)° and 91.25(25)°-95.61(4)°, respectively. The structures obtained for complexes **1** and **2** each represent solvato-polymorphs of structures previously reported by Chiririwa *et al.*[10, 11] (**1**, **2**) and Ashworth *et al.*[12] (**1**). The polymorphs of complex **1** now includes structures containing H_2O (Ashworth, CCDC refcode GAYBAJ), CH_3CN (Chiririwa, CCDC refcode AWOQEJ), and CH_2Cl_2 (this work). Comparison of the structural features of all polymorphs of **1** and **2** shows negligible differences, apart from their unique packing in three dimensions (for molecular overlay and packing diagrams, see Figure S21 and Table S6 in the ESI). In terms of the general structural features of the octahedral complexes, the Ru-C bond lengths of the cyclooctadiene ligands all lie between 2.201(3)-2.231(2) Å (average 2.217(5) Å), where in general a degree of asymmetry is present, leading to one of the Ru-diene bonds to be slightly shorter. This range of bond lengths is comparable to those in other [$RuCl_2$(cod)$(NCR)_2$] analogues (average 2.241(3) Å).[12]

A structural *trans* effect of the cod ligand on the mutually *cis* chlorido ligands (each chlorido is *trans* to a diene bond) has also been described previously.[12] This results in the slight elongation of the Ru-Cl bonds (average 2.420(13) Å), more so than in the related complex [$RuCl_2$(cod)(CO)(NCMe)] previously reported (average 2.395(6) Å),[13] although comparable to corresponding [$RuCl_2$(cod)$(NCR)_2$] complexes (2.407(9)-2.437(1) Å). The Ru-N bonds of the nitrile ligands all fall in a narrow range of 2.021(3)-2.051(3) Å, suggesting a limited effect of the nitrile substituents on the bonding of the nitrile ligands. One feature of the nitrile ligands does stand out: depending on the nitrile substituent, a degree of 'bending' was observed where a deviation from the ideal linear conformation occurs. This distortion, defined by the angles Φ, Ψ, and Ω (Figure 4), includes the effect of bending along the NCR bond, as well as the Ru-N-C_x bond (C_x = sp carbon).

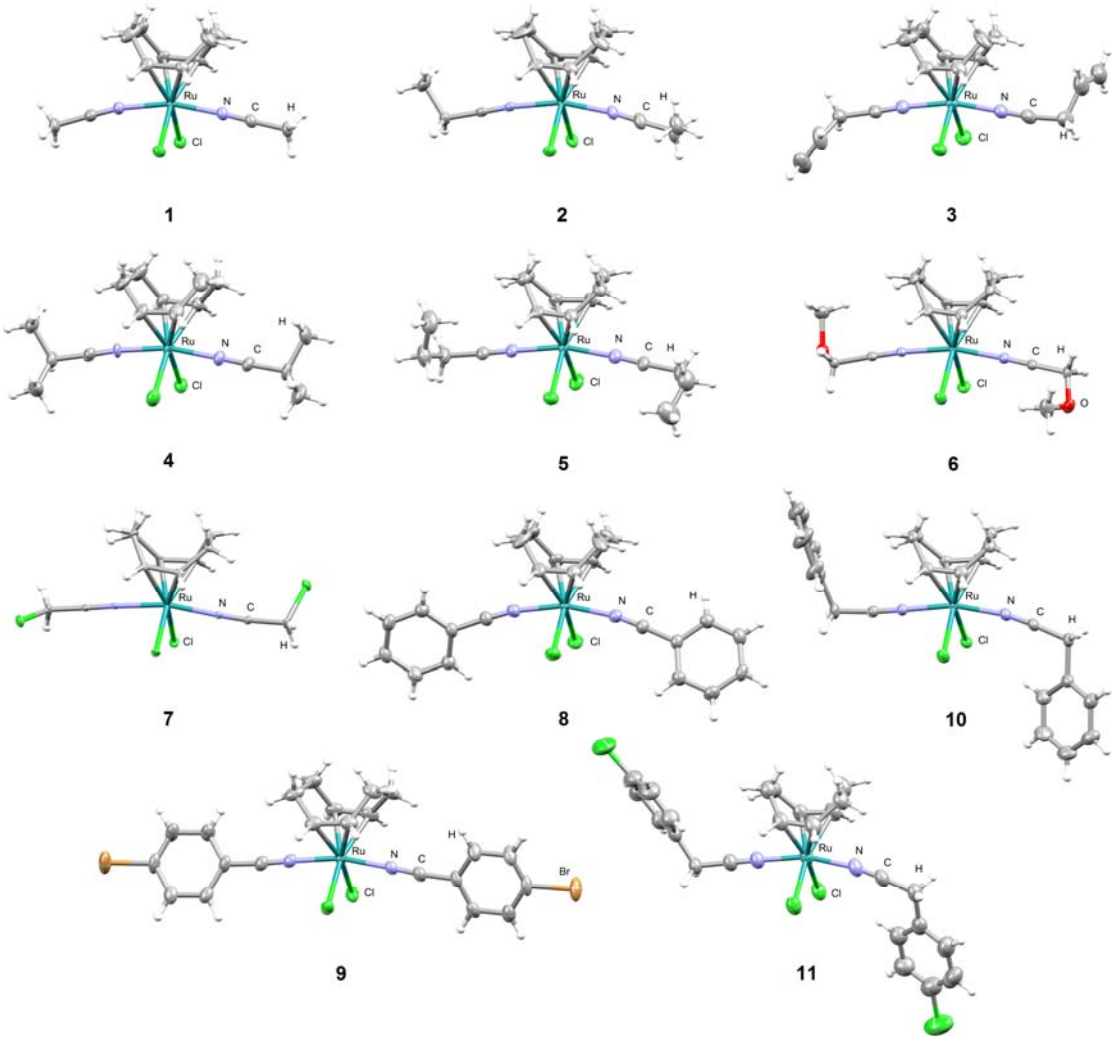

Figure 3. Molecular structures of complexes **1**-**11**. Atomic displacement ellipsoids are presented at 50% probability level. Solvent molecules are omitted for clarity: 2 × CH_2Cl_2 (**1**), $CHCl_3$ (**2**), partial H_2O and $CHCl_3$ (**4**), 2 × MeOH (**9**).

For example, complex **1** containing the least sterically demanding $NCCH_3$ ligands of the series, shows considerable bending with Φ, Ψ, and Ω values of 163.92(11)°, 159.30°, and 157.18°. The complex with the least amount of bending is complex 7, which contains chloroacetonitrile ligands (with Φ, Ψ, and Ω values of 166.85(8)°, 166.19°, and 166.88°). In contrast, the values of Φ, Ψ, and Ω decrease to minima of 162.66(15)°,155.70°, and 150.25° for complex **8**, which contains the bulky phenyl substituents. This is believed to be due the perpendicular conformation of the phenyl rings with respect to the $RuCl_2$(cod) plane that brings about a certain degree of steric hindrance, as well as packing effects in the complete structure (i.e., structures containing solvent molecules (**1**), as opposed to those without (**8**)). A similar effect of nitrile bending was observed in other [$RuCl_2$(cod)$(NCR)_2$] complexes (Φ, Ψ, and Ω values of > 163.15(6)°, 157.64°, and 153.94° belonging to the CH_3CN solvato polymorph of **1** (Chiririwa)), although such extreme distortion is observed in this study for the first time. No mentionable hydrogen bond interactions were observed in the structures of **1**-**11**. The X-ray structure of the dimeric **9b** is shown in Figure 5. In this dimeric structure a pair of Ru(II) centers is bridged by three chlorido ligands with each of the ruthenium centers exhibiting octahedral geometries as part of a pair of face-sharing bioctahedra. An average Ru-cod bond length of 2.208(3) Å corresponds well to the structures discussed above, as well as the [{Ru(cod)(NCR)}(μ_2-Cl)$_3${RuCl(cod)}] congeners (2.163(5)°-2.209(6)°) previously reported.[3, 14]

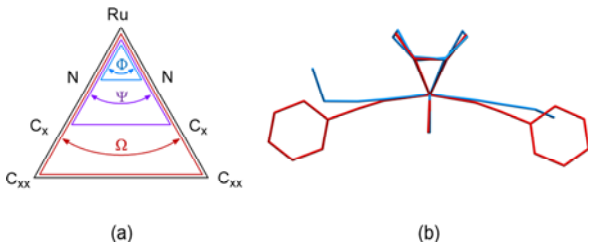

Figure 4. Graphical representation of the bending of nitrile ligands (a), with the structure overlay (b) of the least (complex **7**, blue) and most distorted (complex **8**, red) examples (RMS = 0.0195).

Similarly the Ru-N (2.021(3) Å), Ru-Cl (2.3830(8) Å) and Ru-(μ_2-Cl) (average 2.453(8) Å) bond lengths all fall within the expected ranges of the relevant complexes.[3, 14]

Table 1. Angular parameters (Φ, Ψ, and Ω) in complexes **1**-**11**.

Complex	Φ (°)	Ψ (°)	Ω (°)
7	166.85(8)	166.19	166.88
9	166.1(2)	164.83	166.78
4	165.74(16)	162.79	161.83
6	165.65(9)	163.06	160.80
5	165.42(13)	163.88	164.31
3	165.11(14)	163.24	164.73
10	164.68(7)	161.61	160.16
2	164.03(11)	160.15	158.74
1	163.92(11)	159.45	157.18
11	163.84(14)	159.30	155.90
8	162.66(15)	155.70	150.25

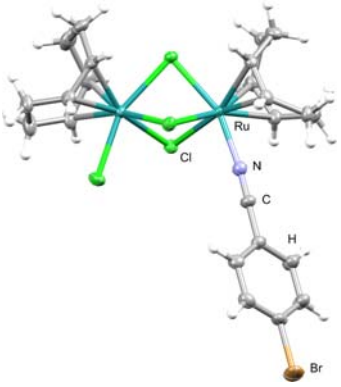

Figure 5. Molecular structure of complex **9b**. Atomic displacement ellipsoids are presented at 50% probability level. One EtOAc solvent molecule is omitted for clarity.

Electrochemistry

The comparative cyclic voltammograms (CVs) at a scan rate of 0.1 V.s^{-1} of complexes **1**-**11** in the 0 V to +1.7 V vs SCE (against FcH/FcH$^+$ couple) is shown in Figure 6, along with a summary of the electrochemical data in Table 2 (see Figures S22 and S23, Table S7 in the ESI for more results). The full scans (in DCM) generally include an oxidation region where a chemically and electrochemically reversible Ru^{II}/Ru^{III} redox couple (between +1.26 and +1.40 V),[15, 16] as well as a chemically and electrochemically irreversible Ru^{III}/Ru^{IV} oxidation process (+1.7 V) are present. In the reduction region an (electro)chemically irreversible reduction process is observed (*c.a.* -1.2 V), which is associated with nitrile ligand reduction.[15] No reoxidation peak or reversibility is observed when the scan was reversed just after the reduction peak. Due to the limited electrochemical window of DCM (-1.7 V to +1.8 V), only the Ru^{II}/Ru^{III} redox couple is considered here. This reversible process is associated with 0.076 V ≤ ΔE ≤ 0.139 V, and 0.076 V ≤ i_{pc}/i_{pa} ≤ 0.139 V at a scan rate of 0.1 V.s^{-1}. The average peak separation of the Ru^{II}/Ru^{III} redox couple is slightly larger than the Nernstian value of 0.059 V for a one electron process due to uncompensated ohmic drops in the cell.[17] An essentially diffusion-controlled electrochemical process is implied through a linear relationship of peak current *vs.* (scan rate)^{½} for the first oxidation and reduction peaks, for scan rates in the regions 0.05 – 1 V.s^{-1} (see ESI). This redox wave becomes electrochemically less reversible at increased scan rates (peak current ratio values in Table S7). A notable effect of the nitrile ligand substituents on the formal reduction potential (E$^{0'}$) of **1**-**11** is seen (Figure 6), with E$^{0'}$ varying between +1.260 V and +1.399 V (scan rate of 0.100 V.s^{-1}). However, no direct relationship between the type of substituent and the magnitude of the redox wave shift is observed. For example, the aromatic phenyl group on benzonitrile exhibits the second lowest E$^{0'}$ (+1.275 V), while its 4'-bromophenyl analogue exhibits the highest E$^{0'}$ (+1.399 V), with the E$^{0'}$ of the aliphatic nitrile complexes falling between these values. In addition, the electron-donating or electron-withdrawing effect of the two nitrile ligands would thus be summative, resulting in the total electron-donating or electron-withdrawing effect for a specific complex. The E$^{0'}$ of complexes **2** and **10** are the same (+1.293 V), indicating that the electronic properties of the ethyl and benzyl groups are comparable. The lowest value of E$^{0'}$ was observed for complex **5** (+1.260 V). The E$^{0'}$ values for the Ru^{II}/Ru^{III} wave obtained for **1**-**11** are in good agreement with those of related Ru(II) nitrile complexes.[15, 16]

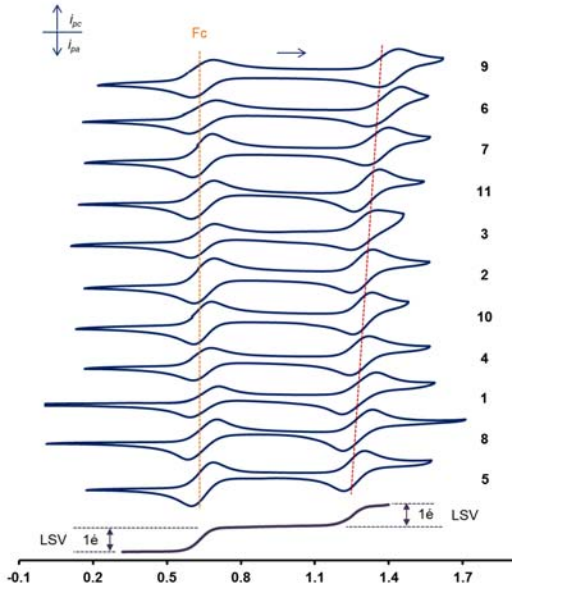

Figure 6. Comparative cyclic voltammograms (between 0 V and +1.7 V vs. FcH/FcH$^+$) at a scan rate of 0.1 V.s^{-1} for complexes **1**-**11**. The red dotted line indicates the Ru^{II}/Ru^{III} redox couple. CVs were measured in 0.1 mol.dm^{-3} [NBu$_4$][PF$_6$]/DCM containing [Ru] = 0.002 mol·dm^{-3} on a glassy carbon working electrode at 25 °C. Bottom: LSV of complex **2** was collected at a scan rate of 0.002 V.s^{-1}.

A linear sweep voltammogram (LSV), obtained using a stationary electrode at a slow scan rate (2 $mV.s^{-1}$) of complex **2** (Figure 6), suggest a one-electron oxidation/reduction process for each of the complexes **1**-**11**.

Table 2. Electrochemical data associated with the Ru^{II}/Ru^{III} redox wave for complexes **1**-**11**.

Complex	Epa	Epc	ΔE	E°'	i_{pa}/i_{pc}
5	1.303	1.217	0.086	1.260	0.94
8	1.336	1.214	0.122	1.275	0.95
1	1.347	1.211	0.136	1.279	0.90
4	1.320	1.242	0.078	1.281	0.97
10	1.331	1.255	0.076	1.293	0.92
2	1.336	1.250	0.086	1.293	0.94
3	1.358	1.243	0.114	1.300	0.83
11	1.364	1.259	0.104	1.312	0.97
7	1.399	1.304	0.095	1.352	0.88
6	1.452	1.313	0.139	1.383	0.90
8	1.440	1.357	0.083	1.399	0.93

DFT study

To gain more insight into the oxidation and reduction processes observed, a density functional theory (DFT) study of complexes **1**-**11** was undertaken. In theory it is possible for each of the complexes to exhibit *cis*/*trans* isomerism with regards to the nitrile and chlorido ligands. Computationally, it was found that the Gibbs free energy of the *cis*-bis(nitrile) complex isomers were comparable with those of the corresponding *trans*-bis(nitrile) complex isomers, with energy differences ($\Delta G_{cis\text{-}trans}$) of between -17.0 $kJ.mol^{-1}$ (lower in energy) and +8.9 $kJ.mol^{-1}$ (higher in energy), which is in the range for the *cis* isomers to experimentally exist. Considering complex **1** as representative example, the molecular orbitals of the neutral **1** (HOMO) and $\mathbf{1}^{+}$ (oxidized **1**, SOMO) species are shown in Figure 7. Electrochemical oxidation involves the removal of an electron from the HOMO of the neutral complex, and therefore the HOMO of the neutral complex as well as the SOMO of the oxidized species (after removal of an electron), suggest the origin of the first oxidation process. The Mulliken spin density plot (Figure 7) of the oxidized complex indicates the most likely position of the remaining unpaired electron of the cation, which in this case shows it is primarily based on the Ru centre. The HOMO of the neutral complex **1** exhibits 40% Ru d_{π} and 58% Cl character, whereas the SOMO of the corresponding oxidized $\mathbf{1}^{+}$ exhibits 36% Ru d_{π}, 27% Cl and 22% cod character. The first oxidation process of the complexes **1**-**11** is hence proposed to be mainly Ru-based, where Ru^{II} is reversibly oxidized to Ru^{III}. The proposal of the following oxidation process at *c.a.* +1.7 V to involve Ru^{III}/Ru^{IV} is supported by the concentration of the HOMO of $\mathbf{1}^{+}$ primarily on the Ru centre (34%).

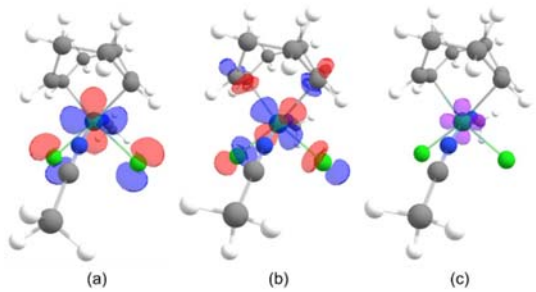

Figure 7. Selected molecular orbitals (red and blue) and Mulliken spin density plots (purple) of **1**: (a) HOMO (neutral), (b) SOMO (oxidized, 1é removal), (c) spin (oxidized, 1é removal).

Similarly, the LUMO of the neutral species **1**, shows a concentration on the metal (37% Ru) as well as nitrile ligands (44%), suggesting a ligand-based reduction. Noteworthy changes in the energy gaps (energy difference between the HOMO and LUMO) of **1**-**11** suggests a distinct difference in chemical reactivity and/or kinetic stability, corresponding to what Pérez-Torrente *et al*.[3] observed from the different rates of reaction depending on the nitrile ligands present. Compounds with smaller energy gaps are usually indicative of less stable and/or more reactive species.[18] In the current range complex **5** showed the largest energy gap (4.56 eV), whereas complex **7** showed the smallest energy gap (1.21 eV), corresponding to the experimental observations where solutions of **7** in halogenated solvents decomposed at a faster rate than the aliphatic-based nitrile-containing complexes **1**-**5**. Interestingly, the small energy gaps of **7** (1.21 eV) and **9** (3.11 eV) also correspond to the low catalytic activity (*vide infra*) of these complexes, although no clear relationship between the calculated energy gaps and associated catalytic activity could be observed.

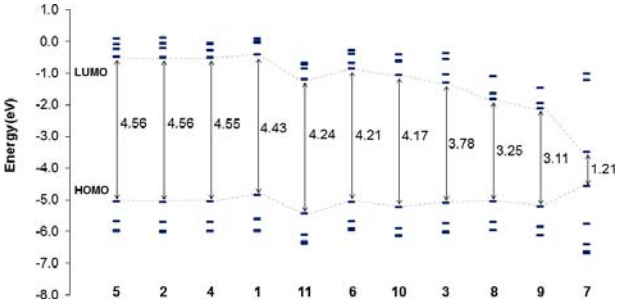

Figure 8. Energy gaps (eV) of complexes **1**-**11**.

Catalysis

Ruthenium-based complexes are known to be catalytically active in an impressive range of C-H,[19, 20] C-C,[19-21] C-N,[21-23] C-O,[21, 23] C-halogen,[20b] N-N,[24, 25] N-H,[20, 26] O-O,[27, 28] O-H,[20, 28] N-O,[29] C-S,[30] S-S,[31] C-Si[28] and C-B[32] transformation reactions. However, no information on the catalytic activity of the Ru-nitrile complexes investigated in this study exists. A screening study was conducted using complex **1** as representative example under the general experimental conditions reported for several commonly studied catalytic reactions (Table 3).

Table 3. Catalytic screening of **1**.

Reaction	Conditions[a]	Conversion (%)	Yield[b] (%)	TON[c]
Carbonyl transfer hydrogenation 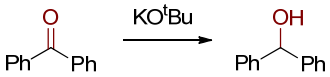	PhCOPh (0.1 mmol), ^{i}PrOH (100 µL), [**1**] = 3 mol%, KO^{t}Bu (10 mol%)	100[d]	>99[d]	33
Alcohol oxidation 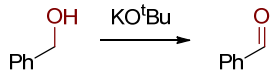	$PhCH_2OH$ (100 µL), [**1**] = 5 mol%, KO^{t}Bu (10 mol%), *p*-$Cl_2C_6H_4$ (10 µL)	18	13	4
Alkyne semihydrogenation 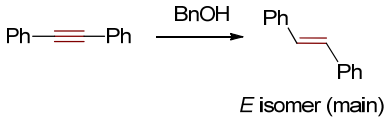 *E* isomer (main)	PhCCPh (0.1 mmol), [**1**] = 5 mol%, BnOH (100 µL), KO^{t}Bu (10 mol%)	22	19	4
Nitrile transfer hydrogenation 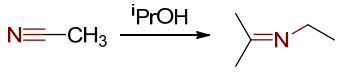	C_2H_5CN (10 µL), ^{i}PrOH (100 µL), [**1**] = 5 mol%, KO^{t}Bu (10 mol%)	28	18	6
Alkene hydrosilylation 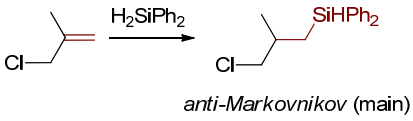 *anti-Markovnikov* (main)	Substrate (0.1 mmol), [**1**] = 5 mol%, H_2SiPh_2 (0.11 mmol), KO^{t}Bu (10 mol%)	59	45	12
Alkyne hydrosilylation 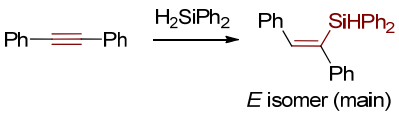 *E* isomer (main)	PhCCPh (0.1 mmol), [**1**] = 5 mol%, H_2SiPh_2 (0.11 mmol)	77 (100)[e]	41 (20)[e]	15 (20)

[a] All reactions (unless otherwise noted) were conducted in C_6D_6 at 80°C over the course of 20 hrs using anisole (same equivalents as substrate) as internal standard in each reaction. [b] NMR yield. [c] Determined at the end of the reaction. [d] After 30 min. [e] Parentheses: addition of KO^{t}Bu (5 mol%).

Complex **1** showed excellent activity in the carbonyl transfer hydrogenation reaction (quantitative conversions), where up to 100% yield was obtained in less than 30 minutes. The other catalytic reactions studied were much less successful. These include the alcohol oxidation (up to 18% conversion), alkyne semihydrogenation (up to 22% conversion), and nitrile transfer hydrogenation (up to 22% conversion) reactions which required substantially longer periods of time (20 hours). Higher activity was observed in the catalytic hydrosilylation of terminal alkenes (up to 59% conversion) and internal alkynes (up to 100% conversion), albeit with low selectivity to the respective silyl products. Based on these results, the catalytic transfer hydrogenation of benzophenone was selected as a model reaction to evaluate the effect of the nitrile ligand in the series of complexes **1**-**11** (Table 4). Complex **1** was found to be the most efficient catalyst able to produce diphenylmethanol nearly quantitatively within 30 min (entry 3), and 79% within the first 10 minutes (TOF = 156 h^{-1}). The efficiency remained high even when the catalyst concentration was reduced to 1 mol% to yield 76% after 30 min (entry 4), and 56% after 10 minutes (TOF = 330 h^{-1}, see Figure S23). A complete conversion to give 100% diphenylmethanol was achieved after 1 hour. The presence of C_6D_6 as solvent also did not affect the efficiency as a duplicate reaction using only ^{i}PrOH gave a conversion of 98% after 30 minutes (aliquot analysed using $CDCl_3$). The addition of base was also critical as only 15% of product was obtained after 30 minutes in the absence of base (entry 2). There was also a strong temperature dependence in the reaction where temperatures below 80°C significantly affected the efficiency of the conversion. For example, only 29% of diphenylmethanol was obtained if the reaction was performed at 50°C (entry 5), and even less (13%, entry 6) if the reaction was performed at room temperature (*ca.* 24°C). Prolonging the reaction to 1 hour only slightly increased the yields to 36% (50°C) and 15% (RT). The performance of the other nitrile complexes **2**-**11** were comparable (TOFs of between 126-154 h^{-1}), except for complexes **6**, **7**, and **9**. In general, yields of 83-96% were obtained (entries 7-10, 13, 15-17) which falls within a 3-15% comparable window. The outliers (entries 11, 12, 14) involve complexes **6**, **7**, and **9**: Complex **6** featured the electron donating OMe group on each nitrile ligand, which may inhibit efficient substrate coordination *via* hydrogen bonding interactions from the lone pairs of the OMe oxygen atoms. In the case of complex **7** the

lowest yield was obtained (16%, entry 12), which is largely ascribed to the instability of the complex in solution, especially at elevated temperatures. Decomposition *via* formation of its dimeric analogue (Figure 2) is not proposed, as enhanced catalytic activity is anticipated (*vide infra*). Complex **9**, featuring the electron-withdrawing 4'-BrPh nitrile ligands, gave rise to a yield of 48% (entry 14), which increased to 87% when using its dimeric analogue, complex **9b** (entry 15). In the case of complex **9b**, a total of two Ru(II) centers per mole of catalyst is present, of which the chlorido-bridges are rapidly cleaved in the presence of suitable ligand donors (substrates) to facilitate efficient catalysis (TOF of 143 h^{-1} as compared to 54 h^{-1}). To confirm the homogeneity of the reactions, a mercury drop test experiment was performed using **1** under optimized conditions (such as those in Table 4, entry 3). After thirty minutes the reaction mixture was a clear solution (apart from base and KCl particles, as well as the mercury drop at the bottom of the tube). A slight decrease in conversion (92% *vs* 99%) was observed and therefore confirms the homogeneous nature of the catalyzed reaction.

Table 4. Transfer hydrogenation of benzophenone using **1**-**11**.

Entry	Complex	[Cat.] (mol%)	Temperature (°C)	Yield[a] (%)	TON[b]	TOF[c] (h^{-1})
1[d]	-	-	80	-	-	-
2[d]	**1**	-	80	15 (0)	5	-
3	**1**	3	80	99 (79)	33	156
4	**1**	1	80	76 (56)	75	330
5	**1**	3	50	29 (24)	10	48
6	**1**	3	RT	13 (7)	4	13
7	**2**	3	80	93 (78)	31	154
8	**3**	3	80	83 (23)	27	45
9	**4**	3	80	90 (71)	30	140
10	**5**	3	80	90 (64)	30	126
11	**6**	3	80	40 (27)	13	54
12	**7**	3	80	16 (10)	5	20
13	**8**	3	80	92 (72)	30	142
14	**9**	3	80	48 (28)	16	54
15	**9b**	3	80	87 (72)	29	143
16	**10**	3	80	95 (73)	31	144
17	**11**	3	80	96 (70)	32	140

General conditions: Ph_2CO (18 mg, 0.1 mmol), $^{i}PrOH$ (100 µL), $KO^{t}Bu$ (10 mol%), Ru catalyst (3 mol%), anisole (11 µl, 0.1 mmol), C_6D_6, 80 °C, 30 min. [a] After 30 min. Parentheses: after 10 min. [b] After 30 min. [c] After 10 min. [d] No base added. Other blank: $KO^{t}Bu$ (10 mol%), no catalyst = 9% yield after 1 hr.

Conclusion

A series of eleven cyclooctadiene Ru(II) complexes of the type $[RuCl_2(cod)(NCR)_2]$ featuring different nitrile ligands were synthesized, fully characterized, and successfully applied as catalysts in six unique transformation reactions. From these catalytic reactions the transfer hydrogenation proves most promising, where complex **1** was the most active pre-catalyst capable of near quantitative conversion within 30 minutes (TOF = 156 h^{-1}). The general activity of most of the complexes evaluated were comparable, which is attributed to the labile nature of the nitrile ligands which enable the facile (de)coordination of substrates to the ruthenium centre. The three complexes **6**, **7** and **9** exhibited the lowest catalytic activity where rapid complex decomposition in solution is a suspected cause. All complexes were electrochemically active, displaying Ru^{II}/Ru^{III} formal potentials ($E^{0'}$) of between +1.303 and +1.440 V. DFT calculations confirmed the locus of the observed Ru^{II}/Ru^{III} formal potentials ($E^{0'}$) to be metal based, and furthermore also revealed a range of calculated energy gaps (4.56-1.21 eV), which help to provide insight into the complex stability/reactivity of each of the compounds. The results therefore indicate that nitrile complexes of Ru(II) that are easily accessed using economic routes, offer a variety of opportunities in the broad field of catalysis. This works broadens the field of Ru(II) nitrile complexes and their associated applications to include more than their current use as versatile synthetic precursors.

Deposition Number(s) 2150078-2150089 contain the supplementary crystallographic data for this paper. These data are provided free of charge by the joint Cambridge Crystallographic Data Center and Fachinformationszentrum Karlsruhe Access Structures service http://www.ccdc.cam.ac.uk/structures.

Supporting Information Summary

Detailed experimental procedures of **1**-**11**, and **9b**, along with NMR spectra, crystallographic data and parameters of all of the complexes, electrochemistry, as well as catalysis data are provided in the Supporting Information.

Acknowledgements

This work has received support from the South African National Research Foundation (Grant nrs. 117995, 138280) and the University of Pretoria. The Centre for High Performance Computing facility (Cape Town) is acknowledged for computer time on their Lengau Cluster.

Conflict of Interest

The author declares no conflict of interest.

Keywords: Cyclic voltammetry • Density functional calculations • Nitrile ligands • Ruthenium • Transfer hydrogenation

[1] (a) R. A. Michelin, M. Mozzon, R. Bertani, *Coord. Chem. Rev.* **1996**, *147*, 299-338. (b) J. Wang, G. Li, Q-s. Li, Y. Xie, R. B. King, *Polyhedron* **2012**, *47*, 165-172.

[2] (a) S. F. Rach, F. E. Kühn, *Chem. Rev.* **2009**, *109*, 2061-2080. (b) C. C. Underwood, B. S. Stadelman, M. L. Sleeper, J. L. Brumaghim, *Inorg. Chim. Acta.* **2013**, *405*, 470-476. (c) T. P. Schlachta, J. F. Schlagintweit, M. R. Anneser, E-M. H. J. Esslinger, M. Muhr, S. Haslinger, F. E. Kühn, *Inorg. Chim. Acta* **2021**, *518*, 120228.

[3] J. J. Pérez-Torrente, C. Cunchillos, D. Gómez-Bautista, M. V. Jiménez, R. Castarlenas, F. J. Lahoz, L. A. Oro, *J. Coord. Chem.* **2012**, *65*, 2981-2991.

[4] B. N. Storhoff, H. C. Lewis, *Coord. Chem. Rev.* **1977**, *23*, 1-29.

[5] (a) V. Y. Kukushkin, A. J. L. Pombeiro, *Chem. Rev.* **2002**, *102*, 1771-1802. (b) M. Vogt, A. Nerush, M. A. Iron, G. Leitus, Y. Diskin-Posner, L. J. W. Shimon, Y. Ben-David, D. Milstein, *J. Am. Chem. Soc.* **2013**, *135*, 17004-17018. (c) T. B. Anisimova, N. A. Bokach, K. V. Luzyanin, M. Haukka, V. Y. Kukushkin, *Dalton Trans.* **2010**, *39*, 10790-10798. (d) G. Wagner, *Inorg. Chim. Acta* **2004**, *357*, 1320-1324.

[6] K. Hiraki, Y. Kinoshita, J. Kinoshita-Kawashima, H. Kawano, *J. Chem. Soc. Dalton Trans.* **1996**, 291-298.

[7] J. López, A. Santos, A. Romero, A. M. Echavarren, *J. Organomet. Chem.* **1993**, *443*, 221-228.

[8] M. R. Kollipara, P. Sarkhel, S. Chakraborty, R. Lalrempuia, *J. Coord. Chem.* **2003**, *56*, 1085-1091.

[9] C. J. Jones, J. A. McCleverty, A. S. Rothin, *J. Chem. Soc. Dalton Trans.* **1986**, 109-111.

[10] H. Chiririwa, R. Meijboom, S. O. Owalude, U. B. Eke, C. Arderne, *Acta Cryst.* **2011**, *E67*, m1096.

[11] H. Chiririwa, R. Meijboom, *Acta Cryst.* **2011**, *E67*, m1335.

[12] T. V. Ashworth, D. C. Liles, D. J. Robinson, E. Singleton, N. J. Coville, E. Darling, A. J. Markwell, *S. Afr. J. Chem.* **1987**, *40*, 183-188.

[13] R. O. Gould, C. L. Jones, D. R. Robertson, T. A. Stephenson, *J. Chem. Soc. Dalton Trans.* **1977**, 129-131.

[14] H. E. Selnau, J. Mahmoud, L. C. Porter, *Inorg. Chim. Acta* **1994**, *224*, 125-129.

[15] N. A. Bokach, M. Haukka, P. Hirva, M. F. C. Guedes Da Silva, V. Y. Kukushkin, A. J. L. Pombeiro, *J. Organomet. Chem.* **2006**, *691*, 2368-2377.

[16] (a) B. A. Babgi, A. M. Asiri, M. N. Arshad, M. G. Humphrey, *J. Coord. Chem.* **2015**, *68*, 1476-1486. (b) M. H. Garcia, P. J. Mendes, M. P. Robalo, M. T. Duarte, N. Lopes, *J. Organomet. Chem.* **2009**, *694*, 2888-2897. (c) J-L. Fillaut, N. N. Dua, F. Geneste, L. Toupet, S. Sinbandhit, *J. Organomet. Chem.* **2006**, *691*, 5610-5618.

[17] N. Elgrishi, K. J. Rountree, B. D. McCarthy, E. S. Rountree, T. T. Eisenhart, J. L. Dempsey, *J. Chem. Educ.* **2018**, *95*, 197-206.

[18] N. Devi, K. Sarma, R. Rahaman, P. Barman, *Dalton Trans.* **2018**, *47*, 4583-4595.

[19] (a) P. B. Arockiam, C. Bruneau, P. H. Dixneuf, *Chem. Rev.* **2012**, *112*, 5879-5918. (b) M. Moselage, J. Li, F. Kramm, L. Ackermann, *Angew. Chem. Int. Ed.* **2017**, 56, 5341-5344. (c) S. Warratz, C. Kornhaaß, A. Cajaraville, B. Niepötter, D. Stalke, L. Ackermann, *Angew. Chem. Int. Ed.* **2015**, 54, 5513-5517. (d) G. Duarah, P. P. Kaishap, T. Begum, S. Gogoi, *Angew. Chem. Int. Ed.* **2019**, *361*, 654-672.

[20] (a) J. F. Hartwig, R. A. Andersen, R. G. Bergman, *J. Am. Chem. Soc.* **1989**, *111*, 2717-2719. (b) F. M. Miloserdov, D. McKay, B. K. Muñoz, H. Samouei, S. A. Macgregor, V. V. Grushin, *Angew. Chem. Int. Ed.* **2015**, *54*, 8466-8470.

[21] I. D. Alshakova, B. Gabidullin, G. I. Nikonov, *ChemCatChem* **2018**, *10*, 4860-4869.

[22] (a) M. Trivedi, S. K. Dubey, G. Kaur, N. P. Rath, *New J. Chem* **2021**, *45*, 17339-17346. (b) W. Wei, H. Yu, A. Zangarelli, L. Ackermann, *Chem. Sci.* **2021**, *12*, 8073-8078.

[23] (a) F. P. Malan, J-H. Noh, G. Naganagowda, E. Singleton, R. Meijboom, *J. Organomet. Chem.* **2016**, *825-826*, 139-145. (b) S. Yadav, N. U. D. Reshi, S. Pal, J. K. Bera, *Catal. Sci. Technol.* **2021**, *11*, 7018-7028.

[24] F. P. Malan, A. Ali, E. Singleton, R. Meijboom, *Inorg. Chim. Acta* **2015**, *437*, 133-142.

[25] C. Kerpal, D. J. Harding, J. T. Lyon, G. Meijer, A. Fielicke, *J. Phys. Chem. C.* **2013**, *117*, 12153-12158.

[26] V. Krishnakumar, B. Chatterjee, C. Gunanathan, *Inorg. Chem.* **2017**, *56*, 7278-7284.

[27] R. Neumann, M. Dahan, *J. Am. Chem. Soc.* **1998**, *120*, 11969-11976.

[28] S. R. Stobart, X. Zhou, R. Cea-Olivares, A. Toscano, *Organometallics* **2001**, *20*, 4766-4768.

[29] J. T. Groves, J. S. Roman, *J. Am. Chem. Soc.* **1995**, *117*, 5594-5595.

[30] K. Matsumoto, H. Sugiyama, *Acc. Chem. Res.* **2002**, *35*, 915-926.

[31] T. Kondo, S-y. Uenoyama, K-i. Fujita, T-a. Mitsudo, *J. Am. Chem. Soc.* **1999**, *121*, 482-483.

[32] T. Sokolnicki, J. Szyling, A. Franczyk, J. Walkowiak, *Adv. Synth. Catal.* **2019**, *362*, 177-183.

Entry for the Table of Contents

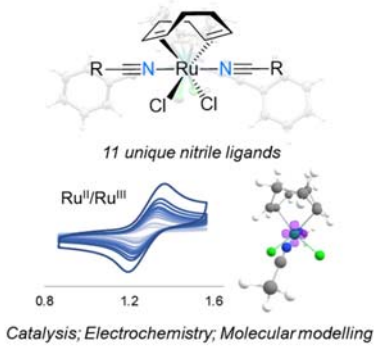

The synthesis and characterization of eleven cyclooctadiene Ru(II) complexes featuring different nitrile ligands are described. Each of these complexes were electrochemically and catalytically active, with the Ru(II) centre able to undergo a reversible Ru^{II}/Ru^{III} oxidation. Among the six different catalytic reactions evaluated, the transfer hydrogenation of benzophenone proved most promising.

Institute and/or researcher Twitter usernames: @frikkiemalan @UPnasagric @ChemistryUP1